PHYSICAL REVIEW E VOLUME 57, NUMBER 3 MARCH 1998

Directed percolation universality in asynchronous evolution of spatiotemporal intermittency

Juri Rolf,* Tomas Bohr,† and Mogens H. Jensen‡
Niels Bohr Institute and Center for Chaos and Turbulence Studies, Blegdamsvej 17, DK-2100 Ø Copenhagen, Denmark
(Received 22 December 1997)

We present strong evidence that a coupled-map-lattice model for spatiotemporal intermittency belongs to the universality class of directed percolation when the updating rules are *asynchronous*, i.e., when only one randomly chosen site is evolved at each time step. In contrast, when the system is subjected to parallel updating, available numerical evidence suggest that it does not belong to this universality class and that it is not even universal. We argue that in the absence of periodic external forcing, the asynchronous rule is the more physical. [S1063-651X(98)50303-0]

PACS number(s): 05.45.+b, 05.70.Jk, 47.27.Cn, 64.60.Ak

The onset of spatiotemporal intermittency is a common phenomenon of many extended systems ranging from models based on coupled-map lattices [1–3] to various experiments in convection [4,5] and in the ''printers instability'' [6,7]. A particular elegant coupled-map lattice (CML) showing spatiotemporal intermittency was introduced some years ago by Chaté and Manneville [1,2]. This CML employs individual maps that can be in two very different states: either in a chaotic (or ''turbulent'') state or in a ''laminar'' state. For a single map the laminar state is ''absorbing'': once the motion is in the laminar state it cannot escape. For the coupled system, one observes interesting dynamical patterns of turbulent patches penetrating into a laminar state, and because of the strong fluctuations, this has been called [1] spatiotemporal intermittency (STI). Once the system is in a pure laminar state, it cannot escape: this is an absorbing state of the full spatially coupled system. These properties of the STI led Pomeau [8] to conjecture that the critical properties at the onset of STI should be governed by the exponents of directed percolation. The turbulent spots of the dynamics in a space-time plot percolate through the system in a manner very similar to the connected bonds in directed percolation (DP), which also has an absorbing state. Subsequent extensive numerical studies and scaling arguments [2,3,9] did not show agreement with this conjecture. On the contrary, it was found that the generic critical properties were not in the universality class of directed percolation. In fact, since the critical properties vary with the parameters, they are not even universal. Nevertheless it was argued in [10] that the apparent nonuniversality is due to traveling solitary excitations with long lifetimes, and that one should in principle recover the DP behavior only for extremely long time scales.

The standard time evolution of a coupled-map lattice is by synchronous (or parallel) updating, in which all individual maps of the lattice are iterated forward simultaneously in a completely deterministic way [11]. The connection between such coupled-map lattices and physical systems, described by partial differential equations is, however, not straightforward. In particular, the synchronous update can only be motivated when the system dynamics is driven by a global periodic external force (or ''clock''). Recently it was observed that the critical properties of a standard CML, using coupled logistic maps, actually depend on whether synchronous or asynchronous updating is applied [12]. Here, asynchronous means that in each step a random site on the CML is chosen and is iterated forward.

This result forces us to reconsider the evidence for nonuniversal behavior for STI, which is all based on the synchronous updating rule. In this Rapid Communication, we thus apply the asynchronous updating to the coupled-map lattice of spatiotemporal intermittency discussed above. We find that all critical exponents, independent of the choice of parameters, fall into the universality class of directed percolation. All critical characteristics of DP, such as hyperscaling, seem to be fulfilled, leading to independent controls of the values of the critical exponents.

The original dynamics of the coupled-map lattice of Chaté and Manneville [1] for a lattice with one space- and one time-direction is written in terms of a field $u_i(t)$ at site i and time t as

$$u_i(t+1)=f(u_i(t))+\frac{\epsilon}{2}\Delta_f u_i(t), \tag{1}$$

where $\Delta_f u_i(t)=f(u_{i-1}(t))-2f(u_i(t))+f(u_{i+1}(t))$. The parameter ϵ measures the strength of the coupling from site i to its two neighbors. The dynamics (1) is parallel or synchronous: all sites are updated at the same time.

The local map f is of the form

$$f(x)=\begin{cases} rx, & \text{if } x\in[0,1/2] \\ r(1-x), & \text{if } x\in[1/2,1] \\ x, & \text{if } x\in]1,r/2]. \end{cases} \tag{2}$$

The chaotic motion of f for $x\leqslant 1$ is governed by a standard tent map of slope r. However, when r exceeds the value 2, the trajectory may escape to a ''laminar'' state with $x>1$, and this state is marginally stable, because the slope in the line of fixed points is 1. As mentioned above, the laminar state is absorbing, i.e., the trajectory cannot be pulled back into the chaotic state. This is no longer the case, when the maps are coupled, since the interactions with its neighbors

*Electronic address: rolfnbi.dk
†Electronic address: tbohrnbi.dk
‡Electronic address: mhjensennbi.dk

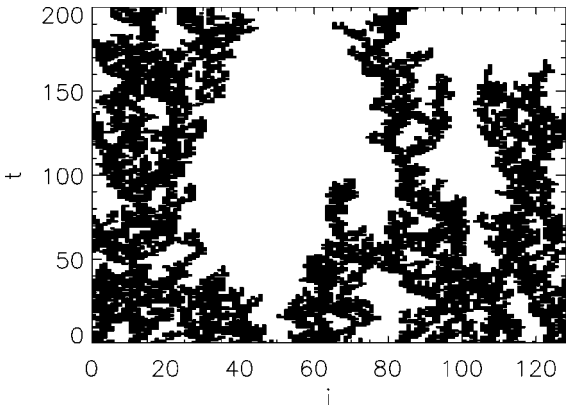

FIG. 1. Time evolution of the asynchronous CML (3) with $r=3.0$, $\epsilon=0.58$ and system size $L=128$. The turbulent sites with $u\leqslant 1$ are black while the laminar sites with $u>1$ are white.

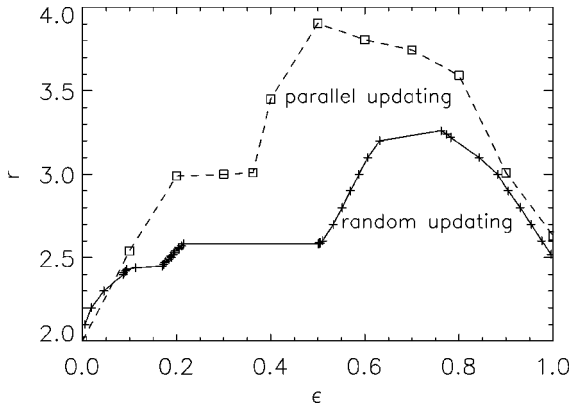

FIG. 2. Phase diagrams of one-dimensional CML for asynchronous updating (crosses) and synchronous updating (boxes).

may pull a laminar site back into chaotic motion, thus causing the interesting interplay between laminar and turbulent regions.

In this work we consider the same CML under asynchronous updating: at time t a random site i_r is selected and is altered according to Eq. (1) while all the other variables keep their values:

$$u_{i_r}(t+1/L)=f(u_{i_r}(t))+\frac{\epsilon}{2}\Delta_f u_{i_r}(t),$$
$$u_i(t+1/L)=u_i(t) \quad \text{for} \quad i\neq i_r, \tag{3}$$

where L is the size of the system. Note that with this choice of time step on average each site is updated once in one unit of time.

The introduction of chaotic iterated maps in extended dynamical systems, and especially simple one-dimensional, noninvertible maps, can only be motivated in a very heuristic way [1]. The closest physical parallel is probably a collection of weakly coupled subunits, each able to perform chaotic dynamics. In order to derive a discrete, local map, one applies a Poincaré section. Note that the Poincaré map owes its simplicity to the fact that it is obtained by restricting the dynamics to a surface through the local phase space and is therefore not in general equivalent to moving the system forward through a fixed time interval. In the absence of an external, periodic forcing, the time interval between consecutive crossings of the section will generically be variable and thus vary from unit to unit in space. To find the state of the entire system at *fixed* time intervals, this variation has to be taken into account. This can, in a rough way, be accomplished by using the asynchronous update in which the units experience slightly different update times. Of course we are thereby replacing the complicated, deterministic update rule by a random one and this is obviously a crude approximation. But we believe that this is often closer to physical reality than the synchronous update. As an example, synchronous updating can lead to complicated, spatial structures, in cellular automata [13], which disappear under asynchronous updating [14], and should therefore be considered unphysical in the absence an external clock.

Figure 1 shows a pattern generated by the asynchronous update introduced above. As only one site is updated at a time, a new horizontal line in the time axis is added only after $L=128$ time steps (i.e., $t\rightarrow t+1$). We observe that the turbulent sites (black in Fig. 1) percolate through the system, sometimes ending in a dangling bond.

To estimate the critical exponents for the randomly updated CML (3), we follow the finite size scaling methods of Houlrik *et al.* [9,15,16]. First of all we have to locate the critical line in the parameter plane (ϵ,r). This is done by measuring the absorption time $\tau(r,\epsilon,L)$, i.e., the time it takes the system starting from a random initial state to reach the absorbing state, averaged over an ensemble of initial conditions. At the critical point $\epsilon=\epsilon_c(r)$, this time diverges like

$$\tau(\epsilon_c,L)\sim L^z, \tag{4}$$

where the usual dynamical exponent $z=\nu_\parallel/\nu_\perp$ has been introduced. Figure 2 shows the phase diagram with the critical line and contrasts it with the critical line for the synchronously updated system (1) taken from [9]. We consider three different values of r and the corresponding values of ϵ_c and z are found in Table I.

The order parameter $m(\epsilon,L,t)$ is defined as the fraction of turbulent sites in the lattice, again averaged over many different initial states [9]. The order parameter scales in the usual way when approaching the critical line from above

$$m\sim(\epsilon-\epsilon_c)^\beta \quad \text{for} \quad \epsilon\rightarrow\epsilon_c^+ \tag{5}$$

TABLE I. Direct measurements of the critical exponents for system (3). The critical values ϵ_c and the exponent z are found simultaneously by approaching the value of ϵ where the scaling (4) is best. The estimation of the other exponents are described in the text. The bottom line shows the directed percolation exponents.

r	ϵ_c	z	β	$\frac{\beta}{\nu_\parallel}$	η
2.2	0.0195(2)	1.58(2)	0.28(1)	0.16(1)	1.51(2)
2.6	0.5096(2)	1.59(2)	0.28(1)	0.16(1)	1.49(2)
3.0	0.5870(3)	1.60(3)	0.28(1)	0.15(2)	1.50(2)
DP		1.57	0.28	0.16	1.51

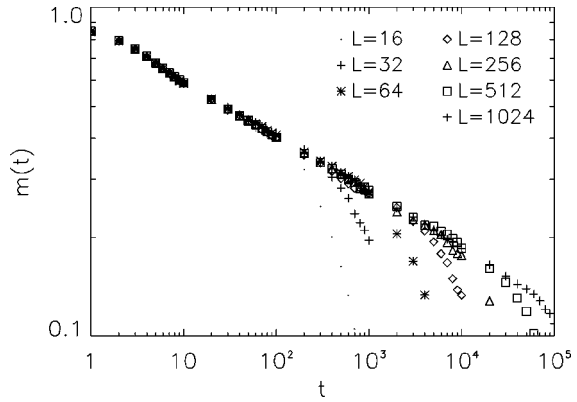

FIG. 3. Order parameter $m(t)$ versus time t for system sizes L between 2^4 and 2^{10} at $r=2.2$. As expected the data falls on one line as long as t is much smaller than the escape time.

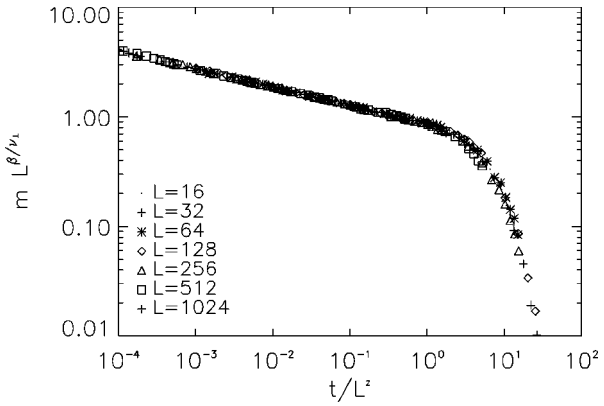

FIG. 4. Rescaling of the order parameter at $r=2.2$ according to (6) to obtain estimates for $\beta/\nu_\perp$ and for z. Data for system sizes L between 2^4 and 2^{10} collapses on one curve.

Using this relation we have estimated the β exponent directly and the results are found in Table I. Applying finite-size scaling arguments we find the following scaling form at the critical point

$$m(\epsilon_c,t,L)\sim L^{-\beta/\nu_\perp} g(t/L^z). \tag{6}$$

The function $g(t/L^z)$ has the following properties: At times much smaller than the absorption time, one expects a power-law decay in time due to critical correlations and the L-dependent prefactor in Eq. (6) must drop out. For $t \ll L^z$, we therefore have

$$m(\epsilon_c,t,L)\sim t^{-\beta/\nu_\parallel}. \tag{7}$$

For times much larger that the absorption time, we may assume uncorrelated decay of the order parameter, and therefore the function g, will decay exponentially. Figure 3 shows a plot of $m(\epsilon_c,t,L)$ versus t at $r=2.2$. The curves for 7 different system sizes in the interval $L=2^4,\ldots,2^{10}$ fall very accurately on the same line in the double logarithmic plot allowing determination of $\beta/\nu_\parallel$ as listed in Table I. As we see in this table all the critical exponents are, within the error bars, consistent with the values for directed percolation, listed at the bottom line in Table I.

In order to obtain independent checks on the values of the critical exponents we have performed a rescaling analysis using Eq. (6). The rescaled curves are shown in Fig. 4. For systems sizes in the interval $L=2^4,\ldots,2^{10}$ the rescaled curves collapse very accurately to a single curve. The corresponding values of $\beta/\nu_\perp$ and z are shown in Table II, again consistent with DP.

TABLE II. Exponents and relations obtained from rescaling analysis using finite size scaling. The fourth column is an estimate of η using the hyperscaling relation (10).

r	$\frac{\beta}{\nu_\perp}$	z	$\eta=2\frac{\beta}{\nu_\perp}+1$	z	η
2.2	0.26(1)	1.57(1)	1.52(2)	1.56(2)	1.53(2)
2.6	0.26(1)	1.57(1)	1.52(2)	1.58(2)	1.49(2)
3.0	0.25(2)	1.58(1)	1.50(3)	1.58(2)	1.53(2)
DP	0.26	1.57	1.51	1.57	1.51

To extract further critical exponents and to check hyperscaling we have looked at the spatial correlations. Even though any dynamics of this CML will end up in the absorbing (laminar) state, it is possible to find nontrivial spatial correlations in a long lasting quasistationary situation [15]. The correlations can be obtained from the pair correlation function

$$C_j(t)=\frac{1}{L}\sum_{i=1}^{L}\langle u_i(t)u_{i+j}(t)\rangle-\langle u(t)\rangle^2, \tag{8}$$

where the brackets denote the average over different initial conditions. If the coupling between the sites is weak, i.e., if ϵ is small, one might expect the spatial correlations to fall off exponentially with distance. At criticality, on the other hand, one expects an algebraic decay of correlations [15]

$$C_j(t)=j^{1-\eta}\psi(j/\xi(t)), \tag{9}$$

where η is the associated critical exponent, and correlations are induced over a length scale $\xi(t)\sim t^{1/z}$ as the CML relaxes towards a steady state. The (equal time) correlation function for various times (at $r=2.2$) is shown in Fig. 5, indicating an algebraic decay in space after long time. The corresponding value of η from this direct measurements is shown in Table

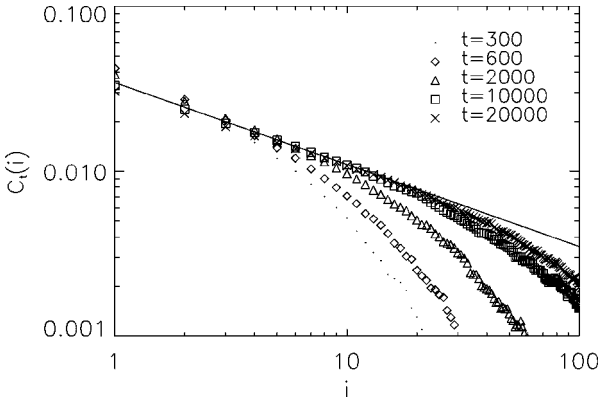

FIG. 5. Spatial correlation function $C_i(t)$ for various times t at $r=2.2$. $C_i(t)$ approaches a straight line with slope $1-\eta$ for large times, indicating an algebraic decay.

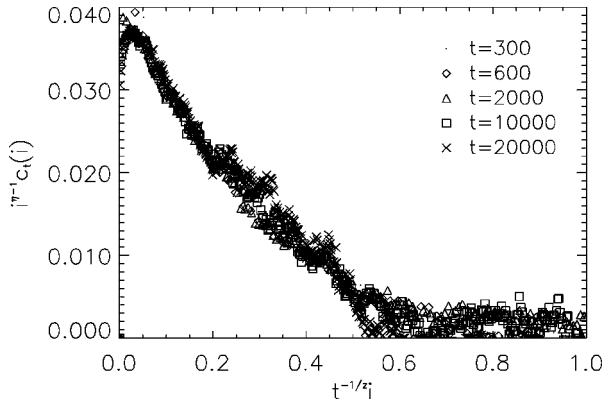

FIG. 6. Rescaled spatial correlation function at $r=2.2$. The data for various times collapses on one curve if the exponents z and η take the values in Table II.

I together with values obtained at other r values. Again the agreement with DP is confirmed.

For the spatial correlations, a rescaling analysis can also be performed by plotting $j/t^{1/z}$ versus $j^{\eta-1}C_j(t)$. Figure 6 shows the corresponding rescaled plot and this technique allows another independent determination of z and η, the values of which are shown in Table II.

The fourth column of Table II contains the values of η obtained from the hyperscaling relation

$$2\beta/\nu = d-2+\eta, \tag{10}$$

giving a third way of estimating the exponent η. All three ways of finding η give results that, within error, are in agreement with the directed percolation value 1.51.

We thus conclude that our numerics gives very strong evidence for the fact that spatiotemporal intermittency in the form of asynchronous coupled maps falls in the universality class of directed percolation. The reason why synchronously updated maps do not behave in a universal way must thus be sought in the complicated correlations built up by the strong constraint of exactly simultaneous, completely deterministic updating, which, in most applications will not be fulfilled. Thus, experiments showing spatiotemporal intermittency should be describable by directed percolation near the transition to turbulence—at least insofar as they do not involve global periodic forcing. One might speculate on the possibility of observing the nonuniversal ''synchronous'' behavior in periodically forced systems, as, say, the printers instability driven by a cylinder of noncircular cross section.

We would like to thank Bernardo Huberman and Benny Lautrup for helpful discussions. J.R. gratefully acknowledges financial support from the Studienstiftung des deutschen Volkes.

[1] H. Chaté and P. Manneville, Physica D **32**, 409 (1988).
[2] H. Chaté and P. Manneville, Physica D **37**, 33 (1989).
[3] H. Chaté, in *Spontaneous Formation of Space-Time Structures and Criticality*, edited by T. Riste and D. Sherrington (Kluwer, Dordrecht, 1991), p. 273.
[4] S. Ciliberto and P. Bigazzi, Phys. Rev. Lett. **60**, 286 (1988).
[5] F. Daviaud, M. Dubois, and P. Bergé, Europhys. Lett. **9**, 441 (1989).
[6] M. Rabaud, S. Michalland, and Y. Couder, Phys. Rev. Lett. **64**, 184 (1990).
[7] S. Michalland and M. Rabaud, Physica D **61**, 197 (1992).
[8] Y. Pomeau, Physica D **23**, 3 (1986).
[9] J. M. Houlrik, I. Webman, and M. H. Jensen, Phys. Rev. A **41**, 4210 (1990).
[10] P. Grasberger and T. Schreiber, Physica D **50**, 177 (1991).
[11] *Theory and Applications of Coupled Map Lattices*, edited by K. Kaneko (Wiley, New York, 1993).
[12] P. Marcq, H. Chaté, and P. Manneville, Phys. Rev. Lett. **77**, 4003 (1996); Phys. Rev. E **55**, 2606 (1997).
[13] M. Nowak and R. M. May, Nature (London) **359**, 826 (1992).
[14] B. A. Huberman and N. S. Glance, Proc. Natl. Acad. Sci. USA **90**, 7716 (1993).
[15] J. M. Houlrik and M. H. Jensen, Phys. Lett. A **16**, 3275 (1992).
[16] J. M. Houlrik and M. H. Jensen, in *Theory and Applications of Coupled Map Lattices*, edited by K. Kaneko (Wiley, New York, 1993), p. 95.